Francois, Alexandre; Himmelhaus, Michael.
Whispering gallery mode biosensor operated in the stimulated emission regime, *Applied Physics Letters*, 2009; 94(3):031101-1.

Whispering gallery mode biosensor operated in the stimulated emission regime

Alexandre Francois[a] and Michael Himmelhaus[b]
Research and Development Division, FUJIREBIO, Inc., 51 Komiya-cho, Hachioji-shi, Tokyo 192-0031, Japan

(Received 28 November 2008; accepted 7 December 2008; published online 20 January 2009)

Whispering gallery modes (WGMs) are generated in fluorescent polymer microparticles in phosphate buffered saline (PBS) above the threshold for stimulated emission and compared to their characteristics below threshold. The WGM microresonators show an eightfold improvement of their signal-to-noise ratio and a threefold increase in their quality factor when operated above threshold. In an investigation on the benefits for biochemical sensing, a real-time adsorption kinetics of *bovine serum albumin* in PBS is monitored and compared with those kinetics acquired by means of a WGM microresonator operated below threshold as well as by surface plasmon resonance (SPR). © *2009 American Institute of Physics*. [DOI: 10.1063/1.3059573]

By monitoring changes in mode positions[1] or bandwidths[2] in response to variations in their immediate environment, optical sensors applying microresonators provide the prospect of high-precision analysis on basis of a phase-sensitive transducer mechanism without the harsh demands on the mechanical precision of interferometers or related kinds of phase-sensitive systems. In fact, most microresonators can be fabricated as robust monolithic blocks that do not require any moving parts for their operation and thus are of high interest for a variety of sensing applications.[3–8]

Among the various kinds of microresonators[9,10] made from semiconducting or dielectric materials those comprising rotational symmetry, such as spheres,[11] cylinders,[12] rings,[13] or toroids,[2,14] have attracted a lot of interest because they can be fabricated from a single material without any need for optical coatings. In such resonators, light is guided by total internal reflection (TIR), which implies that the traveling ray has to impinge onto the resonator/ambient interface with its refractive index contrast $n=n_{\mathrm{res}}/n_{\mathrm{amb}}$ at an angle beyond the critical angle, $\alpha_{\mathrm{crit}}=\arcsin(1/n)$, for TIR. Thus, the light is "whispering" along the boundary between resonator and ambient and returns to its origin after a full round trip, where it must be in phase to achieve constructive interference and thus to allow for the formation of an optical mode. Accordingly, in a simplified picture, the resonance condition for these "whispering gallery modes" (WGMs) reads $m\,\lambda_m = 2\pi \mathrm{n}_{\mathrm{res}} R$, where R is the radius of the plane of travel and λ_m is the wavelength of the WGM with the (integer) mode number m.

Light trapping by TIR entails extremely low losses, which are only due to scattering at bulk and surface imperfections and the curvature of the path of travel. Accordingly, for spheroidal microresonators of not too small size (typically $>100\ \mu$m) very high quality (Q) factors of up to 10^{10} and thus extremely narrow bandwidths $\Delta\lambda_m=\lambda_m/\mathrm{Q}$ can be achieved.[14,15] Therefore, besides the ease of their fabrication, one further advantage of WGM-based sensors is their high resolving power and accordingly low detection limit.[3] For this reason, most optical sensors based on WGM excitations embodied so far have been implemented as microspheres or toroids with diameters of typically some hundreds of micrometers and are made from low loss materials, such as silica[14,15] or CaF_2.[16]

Both the free spectral range $\delta\lambda=\lambda_m-\lambda_{m+1}$ of a spheroidal microresonator and its sensitivity, $\Delta\lambda/\lambda$, i.e., the shift $\Delta\lambda$ in mode position in response to changes in its ambient, scale with $1/R$,[3,17] thereby implying that a reduction in size facilitates mode separation and detection of mode shifts, which in turn aids sensing applications. In particular, unwanted bandwidth broadening due to the higher curvature of smaller resonators and use of materials with higher intrinsic losses, such as polystyrene (PS), may be, at least in a certain size regime, overcompensated by the increased sensitivity $\Delta\lambda/\lambda \propto 1/R$ of such smaller resonators. On this basis, recently also microresonators of a few micrometers in diameter made from silica particles or PS beads have been applied as miniature remote refractometers[7,8] and biosensors.[18–20] In particular, the increased free spectral range $\delta\lambda$ of such smaller resonators enables mode detection and distinction by diffraction optics and therefore allows the excitation of a whole range of modes, for example, by means of the fluorescence emission of embedded semiconductor quantum dots[21] or fluorescent dyes[11] (cf. Fig. 1). This excitation scheme in turn does not only render such sensors into truly radiation controlled and thus remotely operable systems but further increases the information gained, thereby enabling simultaneous determination of resonator parameters and sensing events.[18]

Despite of these obvious advantages, however, the Q factors of such miniature WGM resonators are limited to values of few thousands and thus restrict ultimate sensitivity.[18] As we will discuss in this letter, one way to overcome this limitation is the sensors' operation in the stimulated emission regime, i.e., above the lasing threshold. For the onset of lasing, besides a significant increase of the signal-to-noise (S/N) ratio, also a reduction in bandwidth of the lasing modes is expected, thus improving the detection limit of the sensors. After a brief experimental section (for details see supplemental material),[22] we will first determine the lasing threshold of dye-doped PS beads in an aqueous environment and then explore the benefit of lasing for

[a]Present address: Centre of Expertise in Photonics, School of Chemistry and Physics, The University of Adelaide, Australia 5005.
[b]Electronic mail: ml-himmelhaus@fujirebio.co.jp.

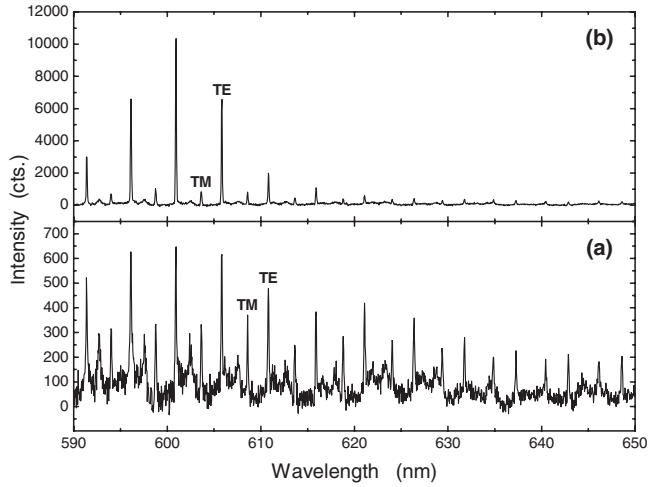

FIG. 1. WGM spectra of a single Nile red-doped PS bead (∅=15 μm) immersed in PBS buffer (a) below and (b) above the lasing threshold, respectively. Acquisition time for both spectra is 1 s; excitation power below threshold 23.2 μW, above threshold 46.4 μW as measured at the objective.

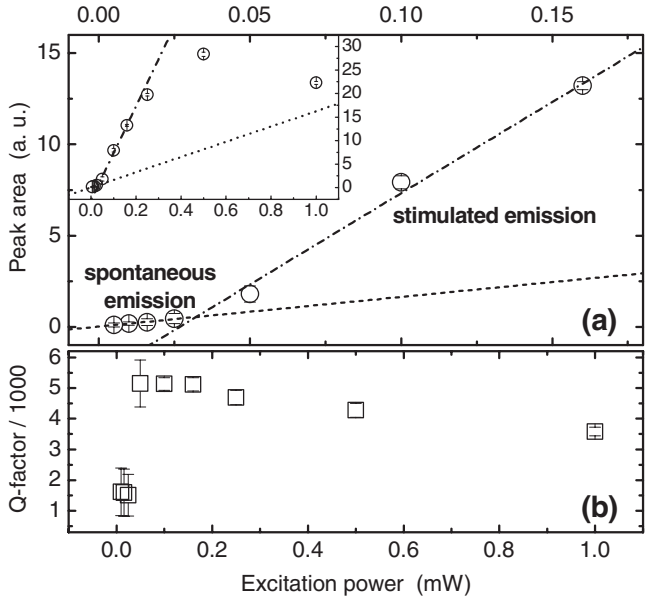

FIG. 2. Lasing threshold of Nile red-doped PS beads pumped at 532 nm at a pulse duration of 9 ps and a pulse repetition rate of 10 kHz: (a) dependence of peak intensity on the excitation power; the dotted and dashed-dotted lines represent linear fits to the two different linear regimes below and above the threshold, respectively, while the inset shows a wider data range. (b) Q factors as determined from the WGM bandwidths and mode positions; data averaged over three experiments.

sensing applications by studying real-time adsorption kinetics of bovine serum albumin (BSA) below and above threshold.

PS beads were doped with Nile red in order to excite WGM from their interior upon optical pumping with a picosecond laser. The doped beads were randomly deposited on a thin glass slide by drop coating. After drying, they were coated with several layers of polyelectrolyte (PE) to fix them on the substrate and to achieve a homogeneously negatively charged surface. Then, the sample was attached to a microfluidic flow cell made of polydimethylsiloxane with a rectangular flow channel of $15\times2\times0.1$ mm^3 in size, which was subsequently filled with phosphate buffered saline (PBS). An inverted microscope was used for both fluorescence excitation and detection. For spectral analysis of the fluorescence emission, a monochromator (600 and 2400 l/mm gratings) and a cooled charge coupled device camera were applied.

Figure 1 displays WGM spectra of one and the same Nile red-doped 15 μm PS bead in PBS buffer excited below [Fig. 1(a)] and above [Fig. 1(b)] the lasing threshold, respectively. Both spectra show a strong modulation of the fluorescence emission of the dye due to the presence of the microresonator, which enhances WGM because of their higher Q factors, i.e., resonator life times, by means of stimulated emission. The spectrum below threshold exhibits the characteristic pairing of first order TM and TE modes of different mode numbers.[7,8] In addition, also some broader resonances, which can be assigned to higher order excitations, are discernible. TE modes have typically higher Q factors than TM modes and for this reason, their lasing threshold is lower as can be seen from Fig. 1(b), where the TM modes are discernible as small peaks only and thus are presumably not lasing under these conditions. The figure shows as obtained raw data, thus allowing a direct comparison of intensities. For the strongest lasing mode in Fig. 1(b), the TE mode at $\lambda=600.92$ nm, the increase I_{st}/I_{sp} in intensity above threshold I_{st} compared to that below threshold I_{sp} [Fig. 1(a)], is 16-fold. To correct for the different excitation power, which was $P_{sp}=23.2$ μW below and $P_{st}=46.4$ μW above threshold, we define an "effective gain" $g_{eff}=(I_{st}/I_{sp})/(P_{st}/P_{sp})$, which yields $g_{eff}=8$ in the present case.

To determine the lasing threshold, the excitation power was systematically varied from 5 μW to 1.0 mW and the corresponding WGM spectra were recorded. Then, the mode exhibiting the highest lasing intensity was selected and fitted via Voigt profiles. Figure 2 displays the resulting dependence of peak intensity (represented by the peak area) and Q factor on the excitation power. The evolution of the peak intensity shows clearly two linear regimes with lower slope below and higher slope above threshold, respectively. Only for excitation powers beyond 0.2 mW deviations from the linear regime could be observed due to dye bleaching as displayed in the inset of Fig. 2(a). Therefore, the threshold could be determined by linear fitting of the two linear regions of spontaneous and stimulated emission as indicated in the figure and subsequent calculation of their intersection, which gave 32 μW, i.e., 32 nJ per laser pulse. In excellent agreement, Yang *et al.*[23] determined the threshold for a toroidal microlaser with similar Q factor in air to 34 μW.

Figure 2(b) illustrates the increase in the Q factor with the onset of lasing of more than a factor of 3, which additionally aids in sensing applications because of the correspondingly increased resolving power of the resonator. Here, with the onset of bleaching above 0.2 mW, a slight reduction is discernible so that it seems to be advisable to operate the sensor not too far above threshold.

As a demonstration of the improved performance of a WGM sensor operated in the stimulated emission regime, the adsorption kinetics of BSA (0.01% in PBS buffer) onto the PS bead surface was monitored in real time at a constant flow rate of 33.75 μl/min. Figure 3 compares the kinetics obtained for (i) a bead operated below the lasing threshold, (ii) one operated above the threshold, and (iii) a reference kinetics as obtained from a surface plasmon resonance (SPR) measurement on a gold surface coated with the same sequence of PE layers as the two PS beads studied. Due to

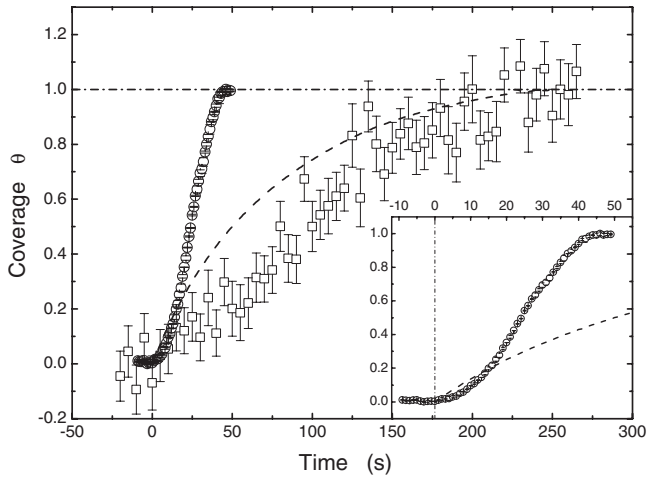

FIG. 3. BSA adsorption kinetics onto PSS-terminated surfaces measured with 15 μm PS beads operated below threshold at 15 μW excitation power (open squares) and above threshold at 55 μW (open circles); for comparison, the result of an SPR measurement performed under the same conditions is shown (dashed line). The inset shows the initial stage of the adsorption process as monitored by a PS bead operated above threshold and SPR, respectively.

different channel cross sections, the SPR flow rate was chosen such that the same volume flux was achieved as in the WGM experiments. The acquisition times for an individual spectrum were set to 0.1 s for WGM spectra above and to 5 s for those below threshold. Despite of this difference of a factor of 50, the kinetics below threshold exhibits high noise, while that above threshold shows a very smooth evolution with a negligible noise comparable to the signal quality of SPR, which performs data collection in 2 s intervals. One should keep in mind, however, that the SPR instrument samples over a macroscopic surface area of about 0.4 mm^2, while the sensor senses an over 500 times smaller area, which also may explain the noise in the measurement below threshold.

Obviously, the kinetics above threshold is much faster than the two other ones. The cause of this difference has not been revealed yet, but might originate either from thermal effects or is related to the higher field strength in the vicinity of the PS bead, which might polarize the molecules and cause their motion toward the bead surface. In any case, as long as the biomolecular function of the molecules is not affected by such effects, an acceleration of an otherwise diffusion-controlled adsorption may be desirable, in particular, for biomedical diagnostics applications. Therefore, we will study these effects in more detail in the future. Further, during the initial adsorption phase, both the WGM kinetics obtained below and above the lasing threshold show a delayed growth in comparison to SPR, as can be seen from the inset of Fig. 3. While the latter resembles basically a Langmuir adsorption kinetics ($k_{ads}=(0.0124\pm5\ 10^{-5})1/s$), the slower response in the case of the WGM sensors indicates a gradual change in BSA concentration, which might have its origin in the use of macroscopic valves and tubing for the WGM experiments. Despite of such open questions, the measurements clearly reveal the improvement of the performance of low-Q WGM biosensors in view of S/N ratio, speed of acquisition, and detection limit.

In conclusion, we have demonstrated that operating WGM sensors above the threshold for stimulated emission yields significant improvements in their S/N ratio (eightfold) and Q factor (threefold) and thus points a way for the development of reliable, sensitive, and fast remote-controlled microscopic optical sensors, which may find ample applications in biomedical diagnostics, microfluidics, and materials science. So far, low-Q WGM sensors based on PS particles and silica spheres operated above the lasing threshold were studied either in air[9,11] or in liquid as refractive index sensors.[6] Now, we were able to show that these systems are also applicable to the detection of thin films of adsorbates in an aqueous environment. In this study on biosensing in the stimulated emission regime, we used somewhat larger particles than in previous work[18–20] because of their higher stability against bleaching. Future activities will therefore aim at a reduction in the sensor diameter, thus further improving the detection limit and versatility of low-Q WGM sensors.

[1]F. Vollmer, D. Braun, A. Libchaber, M. Khoshsima, I. Teraoka, and S. Arnold, Appl. Phys. Lett. **80**, 4057 (2002).
[2]V. S. Ilchenko and L. Maleki, Proc. SPIE **4270**, 120 (2001).
[3]F. Vollmer and S. Arnold, Nat. Methods **5**, 591 (2008).
[4]I. M. White, N. M. Hanumegowda, and X. Fan, Opt. Lett. **30**, 3189 (2005).
[5]M. Gerlach, Y. P. Rakovich, and J. F. Donegan, Opt. Express **15**, 3597 (2007).
[6]Z. Zhang, L. Yang, V. Liu, T. Hong, K. Vahala, and A. Scherer, Appl. Phys. Lett. **90**, 111119 (2007).
[7]P. Zijlstra, K. L. van der Molen, and A. P. Mosk, Appl. Phys. Lett. **90**, 161101 (2007).
[8]S. Pang, R. E. Beckham, and K. E. Meissner, Appl. Phys. Lett. **92**, 221108 (2008).
[9]Y. Yamamoto and R. E. Slusher, Phys. Today **46**(6), 66 (1993).
[10]K. J. Vahala, Nature (London) **424**, 839 (2003).
[11]M. Kuwata-Gonokami, K. Takeda, H. Yasuda, and K. Ema, Jpn. J. Appl. Phys., Part 2 **31**, L99 (1992).
[12]H. J. Moon, G. W. Park, S. B. Lee, K. An, and J. H. Lee, Opt. Commun. **235**, 401 (2004).
[13]C. Y. Chao, W. Fung, and L. J. Guo, IEEE J. Sel. Top. Quantum Electron. **12**, 134 (2006).
[14]D. K. Armani, T. J. Kippenberg, S. M. Spillane, and K. J. Vahala, Nature (London) **421**, 925 (2003).
[15]M. L. Gorodetsky, A. A. Savchenkov, and V. S. Ilchenko, Opt. Lett. **21**, 453 (1996).
[16]I. S. Grudinin, A. B. Matsko, A. A. Savchenkov, D. Strekalov, V. S. Ilchenko, and L. Maleki, Opt. Commun. **265**, 33 (2006).
[17]S. Arnold, M. Khoshsima, I. Teraoka, S. Holler, and F. Vollmer, Opt. Lett. **28**, 272 (2003).
[18]A. Weller, F. C. Liu, R. Dahint, and M. Himmelhaus, Appl. Phys. B: Lasers Opt. **90**, 561 (2008).
[19]A. Francois and M. Himmelhaus, Appl. Phys. Lett. **92**, 141107 (2008).
[20]A. Francois, S. Krishnamoorthy, and M. Himmelhaus, Proc. SPIE **6862**, 686211/1 (2008).
[21]M. V. Artemyev, U. Woggon, and R. Wannemacher, Appl. Phys. Lett. **78**, 1032 (2001).
[22]See EPAPS Document No. E-APPLAB-94-019901 for detailed experimental section. For more information on EPAPS, see http://www.aip.org/pubservs/epaps.html.
[23]L. Yang, D. K. Armani, and K. J. Vahala, Appl. Phys. Lett. **83**, 825 (2003).